



OPEN ACCESS

EDITED BY

Suriya Prakash Muthukrishnan,
All India Institute of Medical Sciences, India

REVIEWED BY

Xinglong Yang,
The First Affiliated Hospital of Kunming
Medical University, China
Jinsoo Koh,
Wakayama Medical University, Japan

*CORRESPONDENCE

Zhenyu Dai
✉ ycsydzy@163.com
Pinglei Pan
✉ panpinglei@163.com

[†]These authors have contributed equally to
this work

RECEIVED 21 December 2024

ACCEPTED 17 March 2025

PUBLISHED 28 March 2025

CITATION

Yang H, Gu S, Sun H, Zhang F, Dai Z and
Pan P (2025) Neural network localization in
Parkinson's disease with impulse control
disorders.
Front. Aging Neurosci. 17:1549589.
doi: 10.3389/fnagi.2025.1549589

COPYRIGHT

© 2025 Yang, Gu, Sun, Zhang, Dai and Pan.
This is an open-access article distributed
under the terms of the [Creative Commons
Attribution License \(CC BY\)](#). The use,
distribution or reproduction in other forums is
permitted, provided the original author(s) and
the copyright owner(s) are credited and that
the original publication in this journal is cited,
in accordance with accepted academic
practice. No use, distribution or reproduction
is permitted which does not comply with
these terms.

Neural network localization in Parkinson's disease with impulse control disorders

Hucheng Yang^{1,2†}, Siyu Gu^{1†}, Haihua Sun^{3†}, Fengmei Zhang²,
Zhenyu Dai^{1*} and Pinglei Pan^{3*}

¹Department of Radiology, The Yancheng School of Clinical Medicine of Nanjing Medical University, Yancheng, China, ²Department of Radiology, Binhai Maternal and Child Health Hospital, Yancheng, China, ³Department of Neurology, The Yancheng School of Clinical Medicine of Nanjing Medical University, Yancheng, China

Background: There is a huge heterogeneity of magnetic resonance imaging findings in Parkinson's disease (PD) with impulse control disorders (ICDs) studies. Here, we hypothesized that brain regions identified by structural and functional imaging studies of PD with ICDs could be reconciled in a common network.

Methods: In this study, an initial systematic literature review was conducted to collect and evaluate whole-brain functional and structural magnetic resonance imaging studies related to PD with ICDs. We subsequently utilized the Human Connectome Project (HCP) dataset ($n = 1,093$) and a novel functional connectivity network mapping (FCNM) technique to identify a common brain network affected in PD with ICDs.

Results: A total of 19 studies with 25 contrasts, incorporating 345 individuals with PD and ICDs, and 787 individuals with PD without ICDs were included in the analysis. By using the HCP dataset and a novel FCNM technique, we ultimately identified that the aberrant neural networks predominantly involve the default mode network (middle and inferior temporal gyrus, anterior cingulate cortex, angular gyrus) and subcortical network (caudate nucleus).

Conclusion: This study suggests that the heterogeneous neuroimaging findings in PD with ICDs can be attributed to shared abnormalities in the default mode and subcortical networks. These dysfunctions are associated with impaired self-regulation, decision-making, and heightened impulsivity in PD with ICDs. Our findings integrate diverse neuroimaging results from previous studies, providing a clearer understanding of the neurobiological mechanisms underlying PD with ICDs at a network level.

KEYWORDS

Parkinson's disease, impulse control disorders, network localization, voxel-based morphometry, functional connectivity network mapping

1 Introduction

Impulse control disorders (ICDs), characterized by compulsive behaviors such as pathological gambling, compulsive shopping, binge eating, and hypersexuality, are notably more prevalent in patients with Parkinson's disease (PD) (Cilia and Van Eimeren, 2011; Weintraub et al., 2015; Voon et al., 2017; Antonini et al., 2017; Fantini et al., 2019). The prevalence of ICDs in the general population is estimated at 0.2–5.3%, but rises considerably to 20–46% among individuals with PD (Weintraub et al., 2015; Corvol et al., 2018). PD patients

with ICDs often suffer from more exacerbated mental health problems correlated with the severity of their ICDs manifestations, resulting in notable personal, familial, and socioeconomic difficulties (Moegle et al., 2020; Dodd et al., 2005; Gan et al., 2021; Voon et al., 2011; Toś et al., 2023). The neural mechanisms underlying PD patients with ICDs are still not fully understood.

Multimodal magnetic resonance imaging (MRI) techniques have been applied to investigate brain functional and structural alterations in various neuropsychiatric diseases (Bowman et al., 2016; Long et al., 2012; Geranmayeh et al., 2014; Amemiya et al., 2024). Taking advantage of neuroimaging techniques, studies have discovered several brain regions that are related to PD with ICDs, with the inferior frontal gyrus, middle and inferior temporal gyri, anterior cingulate cortex (ACC), caudate nucleus, precentral gyrus, and angular gyrus being the relatively more affected (Gan et al., 2021; Esteban-Peñalba et al., 2021; Tessitore et al., 2017a; Maggi et al., 2024; Frosini et al., 2010). However, the findings exhibit significant heterogeneity, likely influenced by variations in study designs or analytical methods (Müller et al., 2018; Lin et al., 2023). Recent studies suggest that neuropsychiatric symptoms and diseases may be more accurately mapped to common brain networks rather than isolated regions (Kletenik et al., 2022; Boes et al., 2015; Cohen et al., 2019; Tetreault et al., 2020; Zhang et al., 2024). This network-based approach shifts the focus from isolated brain regions to a broader brain connectivity framework, benefiting from techniques like functional connectivity network mapping (FCNM) (Kletenik et al., 2022; Joutsa et al., 2022; Fox, 2018; Peng et al., 2022). This approach is conceptually similar to lesion network mapping, which uses lesion locations in patients to identify common networks associated with specific symptoms (Fox, 2018). By integrating neuroimaging data with large-scale brain connectome dataset, researchers can identify common symptom-specific networks underlying various neurological and psychiatric conditions (Kletenik et al., 2022; Boes et al., 2015; Kim et al., 2021; Wawrzyniak et al., 2018). Despite the extensive neuroimaging studies conducted on PD with ICDs, there is still limited research investigating network localization of PD with ICDs.

The objective of our research was to identify brain network disturbances associated with ICDs in PD by integrating results from diverse neuroimaging modalities. Our study utilized the Human Connectome Project (HCP) dataset due to its high-quality and large-scale resting-state functional MRI (fMRI) dataset, which can reduce individual variability and provide more reliable results in network mapping. Initially, we performed a systematic review of existing literature on structural and functional brain abnormalities in PD with ICDs. Next, leveraging large-scale resting-state fMRI dataset from the HCP dataset (Van Essen et al., 2013) and applying the FCNM approach (Mo et al., 2024) to distinct brain networks associated with ICDs in PD, which can enhance our understanding of the neural correlates and offer potential targets for therapeutic interventions.

2 Methods

2.1 Literature search and selection

Adhering to the Preferred Reporting Items for Systematic Reviews and Meta-analyses guidelines (Moher et al., 2009), a comprehensive systematic search was conducted in PubMed, Embase, and Web of

Science to identify relevant studies published until July 30, 2024. We used specific keyword combinations to identify relevant articles: (“Parkinson’s disease” OR “Parkinson”) AND (“impulsive control disorders” OR “pathological gambling” OR “hypersexuality” OR “compulsive eating” OR “compulsive shopping” OR “compulsive buying” OR “punding” OR “compulsive sexual behavior”) AND (“magnetic resonance imaging” OR “neuroimaging” OR “MRI” OR “resting state functional MRI” OR “rs-fMRI” OR “brain connectivity” OR “FC” OR “functional connectivity” OR “ReHo” OR “regional homogeneity” OR “ALFF” OR “amplitude of low frequency fluctuations” OR “fALFF” OR “fractional amplitude of low-frequency fluctuations” OR “cerebral blood flow” OR “CBF” OR “arterial spin labeling” OR “ASL” OR “independent component analysis” OR “ICA” OR “degree centrality” OR “DC” OR “PET” OR “positron emission tomography” OR “SPECT” OR “single photon emission computed tomography” OR “structural magnetic resonance imaging” OR “morphometry” OR “voxel-based” OR “voxel-wise” OR “voxel-based morphometry” OR “VBM” OR “high-resolution imaging” OR “structural neuroimaging” OR “DBM” OR “deformation-based morphometry” OR “GMV” OR “gray matter volume” OR “gray matter” OR “gray matter”). We systematically reviewed relevant meta-analyses and reviews to identify studies potentially omitted from our database search. A flow diagram of the study selection process is shown in [Supplementary Figure S1](#). Studies were considered eligible based on the following inclusion criteria: (1) was published in an English-language peer-reviewed journal as an original article; (2) comparisons of gray matter volume (GMV), task-related activation, or resting-state activity between individuals with PD and ICDs and those with PD without ICDs; (3) analyses conducted voxel-wisely at the whole-brain level; (4) significant results either corrected for multiple comparisons or uncorrected; (5) significant brain cluster coordinates reported in standard reference space (Talairach or Montreal Neurological Institute space [MNI]). Exclusion criteria included: (1) no coordinate system reported; (2) use of region of interest (ROI) analysis: Analyses of local brain function, such as amplitude of low frequency fluctuations (ALFF) and regional homogeneity (ReHo), were conducted at the whole-brain level, without a *a priori* hypotheses. Functional connectivity (FC) analysis was performed using a seed-based approach to investigate whole-brain connectivity patterns, explicitly excluding ROI-to-ROI analyses; (3) all reported coordinates outside the gray matter mask; (4) review or meta-analysis studies. Our analysis concentrated on contrasts rather than studies. Coordinates of peak voxels of significant clusters reported in each contrast were extracted, with coordinates in Talairach space converted to MNI space.

2.2 fMRI data acquisition and preprocessing

We employed the HCP 1200 Subjects Release (S1200) dataset, which contains resting-state fMRI data on healthy young adults 22–37 years of age. In our study, a total of 1,093 healthy adults [594 female; mean (SD) age 28.78 (3.69) years] were included. Exclusion criteria for this dataset included contraindications to MRI, current psychiatric or neurological disorders, use of psychiatric medications within the previous 3 months, pregnancy, and any history of head trauma. Detailed information about the sample is available in a

separate publication (Peng et al., 2022). The demographic details of the HCP are presented in [Supplementary Table S1](#).

The data from the HCP was collected using a 3 T Siemens Trio scanner, ensuring high-resolution imaging for comprehensive analyses. The resting-state fMRI parameters of the HCP dataset are provided in [Supplementary Table S2](#). Participants exhibiting substandard image quality, including visible artifacts or incomplete brain coverage, were excluded from the analysis.

Resting-state fMRI data were preprocessed using SPM12 software¹ and DPABI² (Yan et al., 2016). The first 10 volumes for each participant were discarded to allow the signal to reach equilibrium and the participants to adapt to the scanning noise. The remaining volumes were corrected for the acquisition time delay between slices. Then, realignment was performed to correct the motion between time points. Head motion parameters were computed by estimating the translation in each direction and the angular rotation on each axis for each volume. All participant's data were within the defined motion thresholds (i.e., maximal translational or rotational motion parameters <2 mm or 2°). We also calculated framewise displacement, which indexes the volume-to-volume changes in head position. Several nuisance covariates (linear drift, estimated motion parameters based on the Friston-24 model, spike volumes with framewise displacement >0.5 mm, global signal, white matter signal, and cerebrospinal fluid signal) were regressed out from the data. Because global signal regression can enhance the detection of system-specific correlations and improve the correspondence to anatomical connectivity (Murphy and Fox, 2017), we included this step in the preprocessing of resting-state fMRI data. Then, the datasets were bandpass filtered using a frequency range of 0.01–0.1 Hz. In the normalization step, individual structural images were first coregistered with the mean functional images; the transformed structural images were then segmented and normalized to MNI space using a high-level nonlinear warping algorithm, i.e., the diffeomorphic anatomical registration through the exponentiated Lie algebra technique (Murphy and Fox, 2017). Next, each filtered functional volume was spatially normalized to MNI space using the deformation parameters estimated during the above step and resampled into a 3-mm isotropic voxel. Finally, all data were spatially smoothed with a Gaussian kernel of 6 × 6 × 6 mm³ full width at half maximum.

2.3 Functional connectivity network mapping

The FCNM method was utilized for the construction of networks related to PD with ICDs, delineating brain structural and functional dysfunctional networks by analyzing GMV, task-induced activation, and resting-state activity differences between PD with ICDs and without ICDs. First, 4-mm radius spheres were created at the coordinates of each contrast and merged to form a contrast-specific seed mask, referred to as the contrast seed. Next, using preprocessed resting-state fMRI data from the HCP, we generated a contrast seed to whole brain FC map for each participant by calculating Pearson's

correlation coefficients between the time courses of the contrast seed and every voxel across the brain. These correlation values were then subjected to Fisher's z-transformation to normalize the data. Subsequently, the 1,093 subject-level FC maps were entered into a voxel wise one-sample *t*-test to identify brain regions functionally connected to each contrast seed. Only positive FC values were considered, as the interpretation of negative FC remains controversial (Murphy and Fox, 2017). Group-level *t*-maps were thresholded and binarized at $p < 0.05$, corrected for multiple comparisons using the false discovery rate (FDR) method. Finally, binarized maps of gray matter volume, task-induced activation, and resting-state activity contrasts were overlaid to generate network probability maps, which were thresholded at 60% based on previous well-validated FCNM studies (Zhang et al., 2024; Mo et al., 2024) to define the PD with ICDs task activation, resting-state activity and GMV dysfunctional networks.

2.4 Association with canonical brain networks

To improve interpretability, we examined the spatial relationships PD with ICDs brain dysfunctional networks and 8 well-recognized canonical brain networks. The seven cortical networks were defined as the visual, somatomotor, dorsal attention, ventral attention, limbic, frontoparietal, and default networks according to the Yeo et al. (2011) study. The Human Brainnetome Atlas was utilized to delineate the subcortical network (Fan et al., 2016), encompassing the amygdala, hippocampus, basal ganglia, and thalamus. The spatial association was measured by determining the proportion of overlapping voxels between each PD and ICDs brain dysfunctional network and the corresponding canonical network, normalized by the total voxel count within the canonical network.

3 Results

3.1 Included studies and sample characteristics

Initially, a total of 1,075 relevant documents were identified and then underwent a rigorous screening process; and 19 studies with 25 contrasts, incorporating data from 345 individuals with PD and ICDs, along with 787 individuals with PD without ICDs were finally included in the analysis. These included studies covered a variety of ICDs, including pathological gambling, compulsive shopping, compulsive eating, hypersexuality, binge eating, and punning. This research encompassed 17 functional studies (6 rs-fMRI studies, 5 task-based fMRI studies, 4 PET studies, and 3 SPECT studies) and 2 VBM studies. Details regarding the sample and imaging characteristics of the included studies are summarized in [Table 1](#).

3.2 Abnormal brain networks associated with ICDs in PD

In current study, using the HCP dataset and FCNM technique, we found that the disrupted neural networks predominantly involve the DMN and subcortical network, with specific brain nodes: the

¹ <https://www.fil.ion.ucl.ac.uk/spm/>

² <https://rfmri.org/DPABI>

TABLE 1 Sample and imaging characteristics of the studies included in the analysis.

Study	N (PD-ICDs/PD)	Mean age (SD)	Gender (male)	UPDRS-score	ICDs type	Cognitive status	Imaging modality	Method	Software	Threshold
Cilia et al. (2008)	11/40	57.4 (5.8)	90.9%	UPDRS-III 18 (11)	PG	MMSE: 28.9 (0.8)	SPECT	rCBF	SPM2	$P \leq 0.05$ (FDR)
Frosini et al. (2010)	7/7	57.5 \pm 11	NA	UPDRS-III 15.5 \pm 1.3	PG	MMSE: 29.6	Task fMRI	BOLD	NA	$p \leq 0.01$ (FDR)
Rao et al. (2010)	9/9	56.2 (10.9)	77.8%	NA	PG; CE; CS; BE	MoCA: 27.1 (1.8)	Task fMRI rs-fMRI	rCBF	SPM2	$P \leq 0.05$ (FDR)
van Eimeren et al. (2009)	7/7	60 (9.8)	100%	NA	PG	MoCA: 27.1 (2.5)	PET	rCBF	SPM5	NA
Voon et al. (2011)	14/14	51.5 (8.3)	71.4%	NA	PG	MMSE: 27.7 (3.12)	Task fMRI	BOLD	SPM5	NA
Ray et al. (2012)	7/7	59.7 (10.9)	100%	UPDRS-III 21 (8.04)	PG	NA	PET	rCBF	SPM8	$P \leq 0.05$ (FDR)
Lee et al. (2014)	11/11	56.7 (8.7)	72.7%	UPDRS-III 14.2 (11)	HS; PG; CE; CS; punding	MMSE: 27.7 (1.6)	PET	rCBF	SPM8	NA
Premi et al. (2016)	21/63	65.8 (8.4)	23.8%	UPDRS-III 16.5 (7.2)	CE; PG; HS; punding	MMSE: 27.7 (1.9)	SPECT	rCBF	SPM8	$p < 0.005$
Cilia et al. (2008)	15/15	59.2 (7.6)	93.3%	UPDRS-III 16.9 (8.8)	PG	MMSE: 28.6 (0.9)	SPECT	rCBF	SPM8	$P < 0.05$
Tessitore et al. (2017a)	15/15	57 (9.7)	33.3%	UPDRS-III 15.7 (6)	HS; CE; PG; CS	MMSE:28.8 (8.6) MoCA:24.6 (4.1)	rs-fMRI	FC	SPM12	NA
Tessitore et al. (2017b)	15/15	62.87 (8.6)	86.6%	UPDRS-III 10.9 (4.5)	HS; CE; PG; punding	MMSE: 26.5 (2.2)	rs-fMRI	FC	SPM8	$P \leq 0.05$ (FWE)
Filip et al. (2018)	8/13	65 (5.7)	75%	NA	ICD	NA	Task fMRI	BOLD	SPM12	$P \leq 0.05$ (FWE)
Verger et al. (2018)	18/18	60.4 (67.3)	83.3%	UPDRS-III off 31.9 (12) UPDRS-III on 5.3 (4.1)	PG; HS; CS	NA	PET	rCBF	SPM8	$P < 0.005$
Esteban-Peñalba et al. (2021)	18/17	63.33 (8.24)	88.9%	UPDRS-III 21.5[10–46]	ICD	NA	Task fMRI	BOLD	SPM8	$P \leq 0.05$ (FWE)
Gan et al. (2021)	21/33	59 \pm 9.6	57.1%	UPDRS-III 20.3 \pm 14.2	PG; HS; BE; CS	MMSE: 28.3 \pm 1.1	rs-fMRI	VMHC	SPM8	$p < 0.01$
Kimura et al. (2023)	37/37	66.0 (11.6)	46%	NA	ICD	MMSE: 26.7 (3.9)	rs-fMRI	FC	SPM12	$P < 0.05$
Maggi et al. (2024)	65/287	60.23 \pm 10.45	63%	NA	ICB	MoCA:26.69 \pm 2.49	Structural MRI	VBM	SPM12	$P \leq 0.05$ (FWE)
Baagil et al. (2023)	36/36	65.7 (9.0)	66.6%	UPDRS-III 20.3 (14.1)	ICB	MoCA: 26.7 (3.7)	Structural MRI	VBM	SPM12	$P \leq 0.05$ (FWE)
Theis et al. (2022)	10/10	56.2 (12.37)	80%	UPDRS-III 22.56 (11.48)	HS	MoCA: 27.7 (1.5)	rs-fMRI	BOLD	SPM8	$p < 0.001$

PD, Parkinson's disease; ICDs, impulse control disorders; BOLD, blood oxygen level dependent; FC, functional connectivity; VMHC, voxel-mirrored homotopic connectivity; FDR, false discovery rate; FWE, family-wise error; MMSE, Mini-Mental State Examination; MoCA, Montreal Cognitive Assessment; N, sample size; NA, not applicable; PET, positron emission tomography; rCBF, regional cerebral blood flow; rs-fMRI, resting-state functional magnetic resonance imaging; SPECT, single photon emission computed tomography; UPDRS, Unified Parkinson's Disease Rating Scale; VBM, voxel-based morphometry; SPM, Statistical Parametric Mapping; PG, pathological gambling; CE, compulsive eating; CS, compulsive buying; HS, hypersexuality; BE, binge-eating; ICB: impulse control behaviors.

middle and inferior temporal gyri, ACC, angular gyrus, and caudate nucleus (Figure 1). Additionally, our study revealed that the results obtained using the 1-mm (Supplementary Figure S2) and 7-mm (Supplementary Figure S3) radii closely mirrored those from the 4-mm radius when the FCMN procedure was repeated. The DMN includes regions such as the middle and inferior temporal gyri, ACC, and angular gyrus, with an overlap proportion of 13.2%. The subcortical network primarily includes the caudate nucleus, with an overlap proportion of 24.1% (Figure 2). The overlap proportions with other brain networks, such as visual network, somatomotor network, dorsal attention network, ventral attention network, limbic network, and frontoparietal network, were all <10%. Subsequently, replicating the FCNM procedure with spheres of 1-mm (Supplementary Figure S4) and 7-mm (Supplementary Figure S5) radii, the resulting brain dysfunctional networks closely mirrored those obtained using the 4-mm radius sphere.

4 Discussion

To the best of our knowledge, the current study is the first to use the FCMN method to analyze abnormal brain networks in PD with ICDs. Through the innovative FCNM approach, we analyzed data from 19 studies with 25 contrasts examining a sample of 345 PD patients with ICDs and 787 patients without ICDs, identifying distinct brain networks associated with PD with ICDs across multiple imaging modalities. Our findings revealed that abnormal brain networks mainly involved the DMN, including regions such as the middle and inferior temporal gyri, ACC, and angular gyrus, along with the subcortical network, particularly the caudate nucleus. Network overlap was calculated using a 4-mm radius sphere, and validations with sphere radii of 1 and 7-mm yielded robust and replicable results. These findings indicate that the DMN and subcortical network likely related to the pathogenesis and maintenance of ICDs, offering promising avenues for forthcoming therapeutic strategies.

4.1 Abnormal DMN in PD with ICDs

The DMN is crucial for self-referential processes, social cognition, autobiographical memory, and prospective imagery (Spreng et al., 2009; Wang et al., 2017). It comprises the medial prefrontal cortex, middle and inferior temporal gyri, posterior cingulate cortex, ACC, precuneus, and angular gyrus (Liao et al., 2011; Davey et al., 2016). Studies have indicated that individuals with PD who also exhibit ICDs show disrupted connectivity within the DMN, which may be related to patients focusing more intensely on internal impulses and thoughts, thereby aggravating the symptoms of ICDs (Ma et al., 2011; Morese and Palermo, 2020). Furthermore, altered FC between the DMN, control network, and dorsal attention network may be a key factor contributing to impulsive behavior, making suppression of such behaviors more challenging (Ma et al., 2011; Zhu et al., 2021). Additionally, PD patients with ICDs struggle to effectively suppress DMN activity during task execution, which are believed to contribute to poor decision-making and more prone to impulsive behaviors (Tessitore et al., 2017b; Meyer et al., 2019). Disrupted DMN connectivity in PD patients with ICDs can impair self-referential processing and self-monitoring, reducing their capacity to regulate

internal impulses and promoting impulsive behaviors (Tessitore et al., 2017b; van Eimeren et al., 2009). DMN hyperactivity may indirectly impair self-monitoring capacity by suppressing the executive control network, thereby diverting attention and fostering competition for cognitive resources (Christoff et al., 2009; Sonuga-Barke and Castellanos, 2007). Repetitive transcranial magnetic stimulation (rTMS) has emerged in recent years as a promising non-invasive therapeutic modality for addressing both motor and non-motor symptoms in PD (Wagle Shukla et al., 2016; Aftanas et al., 2020; Brys et al., 2016). Clinical investigations indicate that rTMS targeting prefrontal cortical regions, notably the dorsolateral prefrontal cortex and orbitofrontal cortex, holds promise in mitigating the clinical manifestations of ICDs (Aftanas et al., 2020). Further research has demonstrated that rTMS can elicit improvements in specific cognitive domains in PD with ICDs, notably in areas such as inhibitory control, decision-making, and working memory (Grassi et al., 2021). During dopaminergic treatment in PD patients, aberrant FC across the three networks (DMN, central executive network, and the salience network) linked to the onset of ICDs (Tessitore et al., 2017a; Roussakis et al., 2019; Staubo et al., 2024). The pathological alterations in PD may underlie the emergence of ICDs, with dopamine treatment being intricately linked to both the onset and severity of ICDs (Staubo et al., 2024; Latella et al., 2019).

The middle and inferior temporal gyri play fundamental roles in object recognition, memory integration, language processing, and social cognition, positioning them as key regions for both visual perception and complex cognitive functions (Yeo et al., 2011; Huang et al., 2023; Conway, 2018). Several studies have indicated a significant association between the middle and inferior temporal gyri and ICDs in PD (Roussakis et al., 2019; Carriere et al., 2015; Marques et al., 2021; Zsidó et al., 2019). Structural and functional imaging studies revealed that disruptions in the corticostriatal pathways involving the middle and inferior temporal gyri related to impaired reward processing and ICDs in PD (Roussakis et al., 2019; Carriere et al., 2015; Aracil-Bolaños and Strafella, 2016). Specifically, the middle and inferior temporal gyri are linked to dysfunctional connectivity with regions such as the ACC and ventral striatum, which are central to decision-making and risk evaluation (Marques et al., 2021; Zsidó et al., 2019). These abnormalities are considered fundamental to the emergence of impulsive and compulsive behaviors, such as pathological gambling and hypersexuality, seen in PD patients (Roussakis et al., 2019; Marques et al., 2021).

The ACC is a complex region crucial for emotional regulation, cognitive control, error detection, and autonomic functions, serving as a key integrator of emotional and cognitive processes (Alexopoulos et al., 2008; Reimann et al., 2023; Etkin et al., 2011). Dysfunction in the ACC is linked to heightened impulsivity and diminished cognitive control (Reimann et al., 2023; Etkin et al., 2011). For example, the research conducted by Santangelo et al. (2019) highlighted a notable decrease in functional connectivity within the ACC, indicating a correlation with compromised impulse inhibition (Santangelo et al., 2019). Further research indicates that impairments in the ACC, combined with ventral striatum damage, related to the development of ICDs (Carriere et al., 2015; Paz-Alonso et al., 2020; Probst and van Eimeren, 2013; Filip et al., 2018). In the context of addictive disorders, characterized by heightened impulsivity and compulsive behaviors, the ACC is recognized as a key region involved in regulating these impulsive actions (Goldstein and Volkow, 2011; Koob and Volkow,

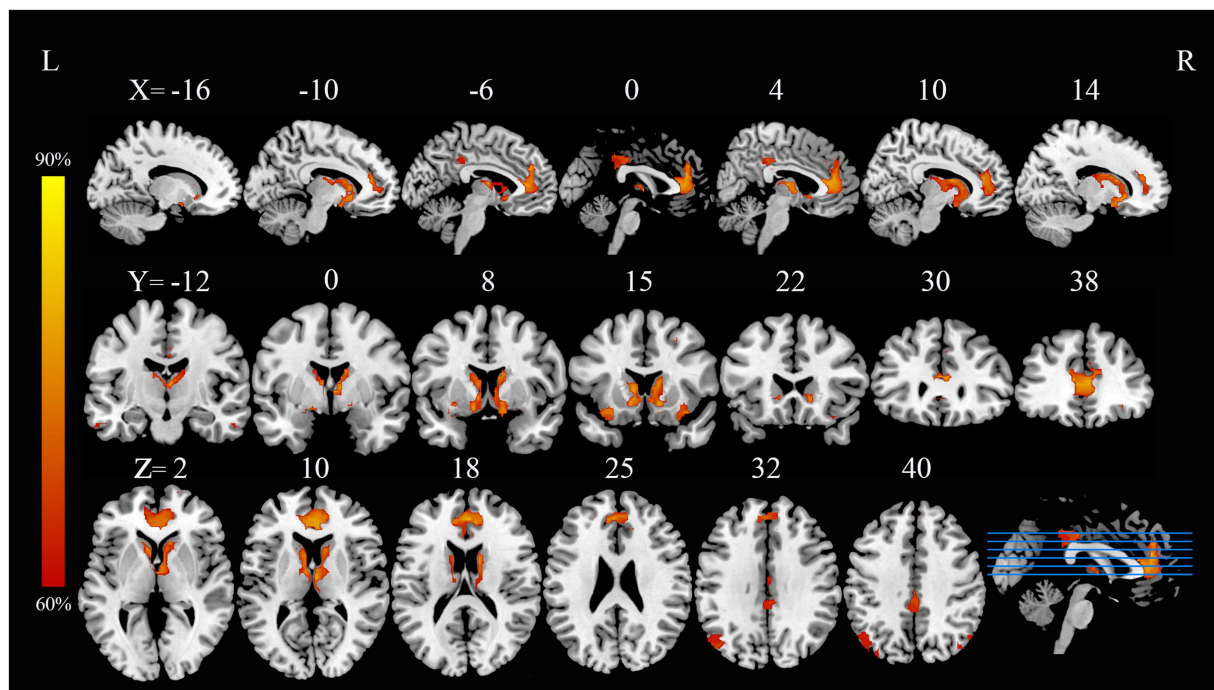


FIGURE 1

PD with ICDs brain dysfunctional networks based on 4-mm radius sphere dysfunctional networks are shown as network probability maps thresholded at 60%, showing brain regions functionally connected to more than 60% of the contrast seeds. PD with ICDs, Parkinson's disease with impulse control disorders.

2016). After TMS treatment in PD with ICDs, it was observed that the treatment could possibly enhance FC between the ACC and various brain regions, especially the prefrontal cortex and limbic system, which may improve emotional regulation and impulse control (Qiu et al., 2023; Balderston et al., 2022). On the other hand, TMS seems to facilitate neuroplasticity in the ACC, suggesting a potential restoration of its functional role in impulse control and an alleviation of impulsive symptoms (Zhang et al., 2021; Vitale et al., 2019).

The angular gyrus integrates multisensory inputs, facilitating semantic processing, episodic memory, and the creation of autobiographical narratives (Milardi et al., 2019; Ji et al., 2019). The angular gyrus, as part of the parietal cortex, processes sensory and motor inputs, making it integral to tasks requiring impulse regulation (Ji et al., 2019; Seghier, 2013; De Micco et al., 2018). Dysfunction of the angular gyrus may result in disturbances within the prefrontal-striatal and midbrain-limbic systems, which are linked to the development of ICDs in PD (Filip et al., 2018; Seghier, 2023). Additionally, dopamine replacement therapy may induce and exacerbate the occurrence of ICD symptoms, which seems to be linked to the overstimulation of the dopamine system in reward pathways, with involvement of the angular gyrus (Cilia and Van Eimeren, 2011; Dalley et al., 2011).

Taken together, our study suggests that ICDs are closely linked to dysfunctional DMN, particularly involving the middle and inferior temporal gyri, ACC, and angular gyrus. These brain regions and the corresponding DMN are associated with self-monitoring and self-regulation, which are significantly involved in the neural mechanisms developing ICDs in PD.

4.2 Abnormal subcortical network in PD with ICDs

The subcortical network is widely distributed and primarily includes the thalamus, caudate nucleus, hippocampus (Milardi et al., 2019; Ji et al., 2019). The subcortical network facilitates essential functions like movement control, emotional regulation, memory processing, and sensory integration, playing a pivotal role in both voluntary actions and automatic bodily functions (Milardi et al., 2019; Zhang et al., 2024; Šimić et al., 2021; Zilverstand et al., 2018). Recently studies have shown that the FC within the subcortical network of PD patients with ICDs undergoes significant alterations (Gan et al., 2021; Esteban-Peñalba et al., 2021; Petersen et al., 2018).

The caudate nucleus was identified as an important node in the subcortical network in patients with PD with ICDs in our study. The caudate nucleus, a critical component of the basal ganglia, is fundamentally involved in regulating a range of physiological processes, including motor control, learning, and higher cognitive functions (Zhang et al., 2024; Šimić et al., 2021; Grahn et al., 2009). ICDs in PD patients have been found to be connected to aberrant FC the caudate nucleus, possibly involving brain regions associated with emotion, cognition, and sensation (Zilverstand et al., 2018; Hepp et al., 2017). Neuroimaging research shows that dopamine agonists like pramipexole heighten impulsivity by influencing the anterior caudate, which governs impulsive choices (Lee et al., 2014; Martinez et al., 2020; Williams and Potenza, 2008). Moreover, the inhibitory control between the prefrontal cortex and the caudate nucleus is weakened in these patients, related to impulsive decision-making and behaviors (De Micco et al., 2018). Disruption of the regulatory balance within the subcortical-cortical

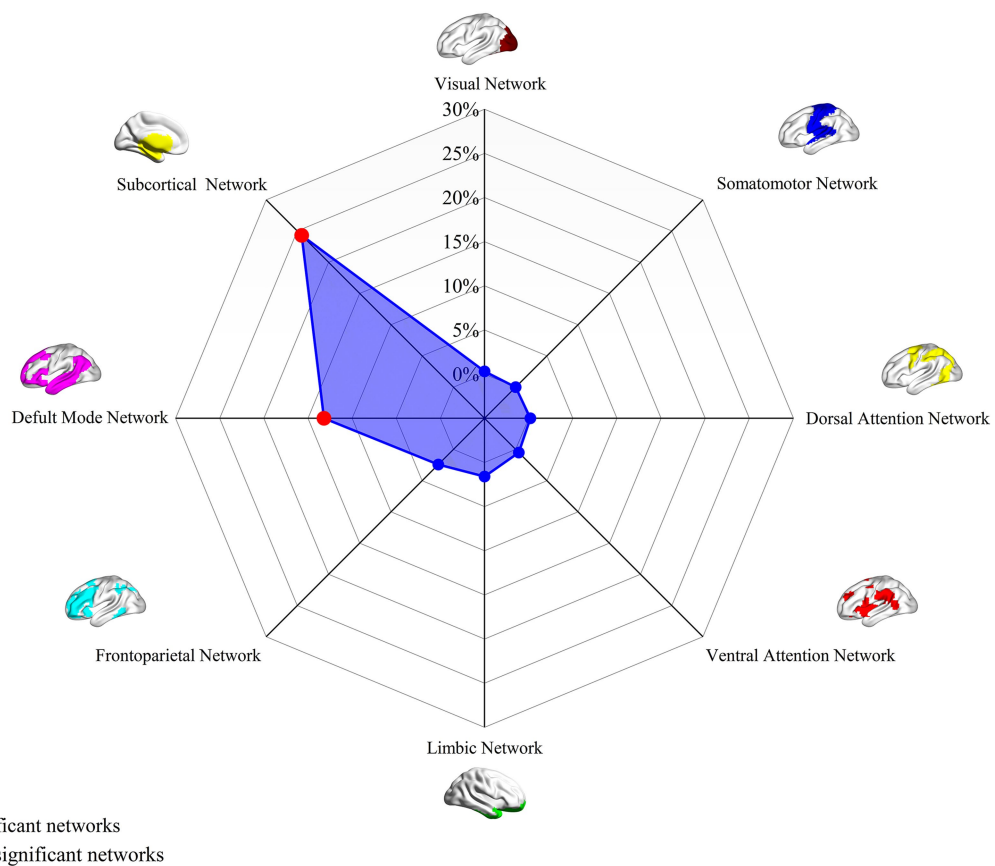


FIGURE 2 Associations of dysfunctional brain networks with canonical brain networks in PD with ICDs based on 4-mm radius sphere. Polar plots display the proportion of overlapping voxels between each brain dysfunctional network and a canonical network relative to all voxels within the corresponding canonical network. The red circles represent brain dysfunction networks, defined as significant networks, exhibiting $\geq 10\%$ overlap with canonical networks, whereas the blue circles represent non-significant networks with $< 10\%$ overlap. PD with ICDs, Parkinson’s disease with impulse control disorders.

circuits is believed to be a key factor of the emergence of ICDs in PD (Kelly et al., 2020). Impairments in the connectivity between the caudate and cortical regions further drive impulsive behaviors (De Simoni et al., 2018). Additionally, lower dopamine transporter binding in the caudate is linked to greater impulsivity, suggesting its role in controlling inhibitory actions (Smith et al., 2018; London, 2020; Bu et al., 2021).

Ultimately, much like the DMN, the subcortical network is integral to the development of ICDs in PD. The abnormality of the caudate nucleus may disrupt neural circuits responsible for regulating impulsivity, which is associated with ICDs. Dysfunctions in subcortical network may relate to the dysregulation of inhibitory control and increased impulsivity, which making patients prone to ICDs like pathological gambling, hypersexuality, and compulsive shopping (Meyer et al., 2020).

4.3 Limitations and future perspectives

There are several limitations to this study. First, to identify brain network localization of PD with ICDs, we utilized resting-state fMRI data from a large sample of healthy adults provided by the HCP dataset. Since the HCP dataset consists of young healthy adults, it may not comprehensively reflect the network alterations associated with PD

and ICDs, which could arise from aging, disease progression, or pharmacological interventions. It might be more suitable to use data more closely matching the demographic and clinical profiles of the patients featured in the selected studies. Second, given the limitations of previous research, we utilized multimodal neuroimaging data rather than a single modality, each with distinct physiological significance, which may have influenced the results; future studies employing single modalities separately could enhance accuracy in network localization. Third, Although the FCNM approach effectively identified common networks associated with PD and ICDs, subtle variations in network dysfunction may exist among different ICDs subtypes. Future studies with larger sample sizes and more detailed clinical phenotyping could investigate potential subtype-specific network signatures. Fourth, it is crucial to emphasize that our findings reveal a correlational relationship between the identified brain networks and this disorder. While these networks likely contribute to understand the pathophysiology of ICDs, our research is unable to determine the causal relationship between the current disease and the dysfunctional networks. Future longitudinal studies are needed to clarify the causal relationship between the current disease and network changes. Finally, drawing on the study discoveries regarding abnormal brain networks, upcoming research could integrate brain stimulation methods such as TMS or transcranial direct current stimulation to specifically address and regulate the deviant

connections within the DMN and subcortical networks. This approach is designed to alleviate symptoms linked to ICDs.

5 Conclusion

In conclusion, our study utilized the novel FCNM approach with large-scale human brain connectome data to pinpoint brain structural and functional heterogeneity within brain functional networks in patients with ICDs in PD. Our study identified specific brain networks associated with ICDs symptoms, predominantly the DMN, which encompasses brain regions like the middle and inferior temporal gyri, ACC, and angular gyrus, and the subcortical network, which involves the caudate nucleus. These findings may help resolve inconsistencies in previous neuroimaging studies and enhance our understanding of the neurobiological mechanisms underlying PD with ICDs from a network-level perspective.

Data availability statement

The raw data supporting the conclusions of this article will be made available by the authors, without undue reservation.

Author contributions

HY: Data curation, Formal analysis, Investigation, Methodology, Software, Visualization, Writing – original draft. SG: Data curation, Methodology, Project administration, Software, Supervision, Validation, Writing – review & editing. HS: Funding acquisition, Resources, Supervision, Writing – review & editing. FZ: Resources, Supervision, Writing – review & editing. ZD: Conceptualization, Funding acquisition, Supervision, Writing – review & editing. PP: Conceptualization, Funding acquisition, Writing – review & editing.

Funding

The author(s) declare that financial support was received for the research and/or publication of this article. This work was supported by the Jiangsu Commission of Health (LKZ2023019 and ZD2022009) and Yancheng Commission of Health (YCBK202216).

Acknowledgments

We would like to thank the team of JiaJia Zhu from The First Affiliated Hospital of Anhui Medical University for providing the technical support.

Conflict of interest

The authors declare that the research was conducted in the absence of any commercial or financial relationships that could be construed as a potential conflict of interest.

Generative AI statement

The authors declare that no Gen AI was used in the creation of this manuscript.

Publisher's note

All claims expressed in this article are solely those of the authors and do not necessarily represent those of their affiliated organizations, or those of the publisher, the editors and the reviewers. Any product that may be evaluated in this article, or claim that may be made by its manufacturer, is not guaranteed or endorsed by the publisher.

Supplementary material

The Supplementary material for this article can be found online at: <https://www.frontiersin.org/articles/10.3389/fnagi.2025.1549589/full#supplementary-material>

SUPPLEMENTARY FIGURE S1

A flow diagram of the study selection process. Analyses of local brain function, such as ALFF and ReHo, were conducted at the whole-brain level, without a priori hypotheses. FC analysis was performed using a seed-based approach to investigate whole-brain connectivity patterns, explicitly excluding ROI-to-ROI analyses. ALFF, amplitude of low-frequency fluctuations; FC, functional connectivity; GM, gray matter; PD with ICDs, Parkinson's disease with impulse control disorders; ReHo, regional homogeneity; ROI, region of interest VBM, voxel-based morphometry.

SUPPLEMENTARY FIGURE S2

PD with ICDs brain dysfunctional networks based on 1-mm radius sphere. Dysfunctional networks are shown as network probability maps thresholded at 60%, showing brain regions functionally connected to more than 60% of the contrast seeds. PD with ICDs, Parkinson's disease with impulse control disorders.

SUPPLEMENTARY FIGURE S3

PD with ICDs brain dysfunctional networks based on 7-mm radius sphere. Dysfunctional networks are shown as network probability maps thresholded at 60%, showing brain regions functionally connected to more than 60% of the contrast seeds. PD with ICDs, Parkinson's disease with impulse control disorders.

SUPPLEMENTARY FIGURE S4

Associations of dysfunctional brain networks with canonical brain networks in PD with ICDs based on 1-mm radius sphere. Polar plots display the proportion of overlapping voxels between each brain dysfunctional network and a canonical network relative to all voxels within the corresponding canonical network. The red circles represent brain dysfunction networks, defined as significant networks, exhibiting $\geq 10\%$ overlap with canonical networks, whereas the blue circles represent non-significant networks with $<10\%$ overlap. PD with ICDs, Parkinson's disease with impulse control disorders.

SUPPLEMENTARY FIGURE S5

Associations of dysfunctional brain networks with canonical brain networks in PD with ICDs based on 7-mm radius sphere. Polar plots display the proportion of overlapping voxels between each brain dysfunctional network and a canonical network relative to all voxels within the corresponding canonical network. The red circles represent brain dysfunction networks, defined as significant networks, exhibiting $\geq 10\%$ overlap with canonical networks, whereas the blue circles represent non-significant networks with $<10\%$ overlap. PD with ICDs, Parkinson's disease with impulse control disorders.

References

- Aftanas, L. I., Brack, I. V., Kulikova, K. I., Filimonova, E. A., Dzemidovich, S. S., Piradov, M. A., et al. (2020). Clinical and neurophysiological effects of dual-target high-frequency rTMS over the primary motor and prefrontal cortex in Parkinson's disease. *Zh. Nevrol. Psikhiatr. Im. S S Korsakova* 120, 29–36. doi: 10.17116/jnevro202012005129
- Alexopoulos, G. S., Gunning-Dixon, F. M., Latoussakis, V., Kanellopoulos, D., and Murphy, C. F. (2008). Anterior cingulate dysfunction in geriatric depression. *Int. J. Geriatr. Psychiatry* 23, 347–355. doi: 10.1002/gps.1939
- Amemiya, S., Takao, H., and Abe, O. (2024). Resting-state fMRI: emerging concepts for future clinical application. *J. Magn. Reson. Imaging* 59, 1135–1148. doi: 10.1002/jmri.28894
- Antonini, A., Barone, P., Bonuccelli, U., Annoni, K., Asgharnejad, M., and Stanzione, P. (2017). ICARUS study: prevalence and clinical features of impulse control disorders in Parkinson's disease. *J. Neurol. Neurosurg. Psychiatry* 88, 317–324. doi: 10.1136/jnnp-2016-315277
- Aracil-Bolaños, I., and Strafella, A. P. (2016). Molecular imaging and neural networks in impulse control disorders in Parkinson's disease. *Parkinsonism Relat. Disord.* 22, S101–S105. doi: 10.1016/j.parkreldis.2015.08.003
- Baagil, H., Hohenfeld, C., Habel, U., Eickhoff, S. B., Gur, R. E., Reetz, K., et al. (2023). Neural correlates of impulse control behaviors in Parkinson's disease: Analysis of multimodal imaging data. *Neuroimage Clin.* 37:103315. doi: 10.1016/j.nicl.2023.103315
- Balderston, N. L., Beer, J. C., Seok, D., Makhoul, W., Deng, Z. D., Girelli, T., et al. (2022). Proof of concept study to develop a novel connectivity-based electric-field modelling approach for individualized targeting of transcranial magnetic stimulation treatment. *Neuropsychopharmacology* 47, 588–598. doi: 10.1038/s41386-021-01110-6
- Boes, A. D., Prasad, S., Liu, H., Liu, Q., Pascual-Leone, A., Caviness, V. S. Jr., et al. (2015). Network localization of neurological symptoms from focal brain lesions. *Brain* 138, 3061–3075. doi: 10.1093/brain/awv228
- Bowman, F. D., Drake, D. F., and Huddleston, D. E. (2016). Multimodal imaging signatures of Parkinson's disease. *Front. Neurosci.* 10:131. doi: 10.3389/fnins.2016.00131
- Brys, M., Fox, M. D., Agarwal, S., Biagioni, M., Dacpano, G., Kumar, P., et al. (2016). Multifocal repetitive TMS for motor and mood symptoms of Parkinson disease: a randomized trial. *Neurology* 87, 1907–1915. doi: 10.1212/wnl.0000000000003279
- Bu, M., Farrer, M. J., and Khoshbouei, H. (2021). Dynamic control of the dopamine transporter in neurotransmission and homeostasis. *NPJ Parkinsons Dis.* 7:22. doi: 10.1038/s41531-021-00161-2
- Carriere, N., Lopes, R., Defebvre, L., Delmaire, C., and Dujardin, K. (2015). Impaired corticostriatal connectivity in impulse control disorders in Parkinson disease. *Neurology* 84, 2116–2123. doi: 10.1212/wnl.0000000000001619
- Christoff, K., Gordon, A. M., Smallwood, J., Smith, R., and Schooler, J. W. (2009). Experience sampling during fMRI reveals default network and executive system contributions to mind wandering. *Proc. Natl. Acad. Sci. U. S. A.* 106, 8719–8724. doi: 10.1073/pnas.0900234106
- Cilia, R., Siri, C., Marotta, G., Isaias, I. U., De-Gaspari, D., Canesi, M., et al. (2008). Functional abnormalities underlying pathological gambling in Parkinson disease. *Arch. Neurol.* 65, 1604–11. doi: 10.1001/archneur.65.12.1604
- Cilia, R., and Van Eimeren, T. (2011). Impulse control disorders in Parkinson's disease: seeking a roadmap toward a better understanding. *Brain Struct. Funct.* 216, 289–299. doi: 10.1007/s00429-011-0314-0
- Cohen, A. L., Soussand, L., Corrow, S. L., Martinaud, O., Barton, J. J. S., and Fox, M. D. (2019). Looking beyond the face area: lesion network mapping of prosopagnosia. *Brain* 142, 3975–3990. doi: 10.1093/brain/awz332
- Conway, B. R. (2018). The organization and operation of inferior temporal cortex. *Annu. Rev. Vis. Sci.* 4, 381–402. doi: 10.1146/annurev-vision-091517-034202
- Corvol, J. C., Artaud, F., Cormier-Dequaire, F., Rascol, O., Durif, F., Derkinderen, P., et al. (2018). Longitudinal analysis of impulse control disorders in Parkinson disease. *Neurology* 91, e189–e201. doi: 10.1212/wnl.0000000000005816
- Dalley, J. W., Everitt, B. J., and Robbins, T. W. (2011). Impulsivity, compulsivity, and top-down cognitive control. *Neuron* 69, 680–694. doi: 10.1016/j.neuron.2011.01.020
- Davey, J., Thompson, H. E., Hallam, G., Karapanagiotidis, T., Murphy, C., De Caso, I., et al. (2016). Exploring the role of the posterior middle temporal gyrus in semantic cognition: integration of anterior temporal lobe with executive processes. *NeuroImage* 137, 165–177. doi: 10.1016/j.neuroimage.2016.05.051
- De Micco, R., Russo, A., Tedeschi, G., and Tessitore, A. (2018). Impulse control behaviors in Parkinson's disease: drugs or disease? Contribution from imaging studies. *Front. Neurol.* 9:893. doi: 10.3389/fneur.2018.00893
- De Simoni, S., Jenkins, P. O., Bourke, N. J., Fleminger, J. J., Hellyer, P. J., Jolly, A. E., et al. (2018). Altered caudate connectivity is associated with executive dysfunction after traumatic brain injury. *Brain* 141, 148–164. doi: 10.1093/brain/awx309
- Dodd, M. L., Klos, K. J., Bower, J. H., Geda, Y. E., Josephs, K. A., and Ahlskog, J. E. (2005). Pathological gambling caused by drugs used to treat Parkinson disease. *Arch. Neurol.* 62, 1377–1381. doi: 10.1001/archneur.62.9.noc50009
- Esteban-Peñalba, T., Paz-Alonso, P. M., Navalpotro-Gómez, I., and Rodríguez-Oroz, M. C. (2021). Functional correlates of response inhibition in impulse control disorders in Parkinson's disease. *Neuroimage Clin.* 32:102822. doi: 10.1016/j.nicl.2021.102822
- Etkin, A., Egner, T., and Kalisch, R. (2011). Emotional processing in anterior cingulate and medial prefrontal cortex. *Trends Cogn. Sci.* 15, 85–93. doi: 10.1016/j.tics.2010.11.004
- Fan, L., Li, H., Zhuo, J., Zhang, Y., Wang, J., Chen, L., et al. (2016). The human Brainnetome atlas: a new brain atlas based on connective architecture. *Cereb. Cortex* 26, 3508–3526. doi: 10.1093/cercor/bhw157
- Fantini, M. L., Durif, F., and Marques, A. (2019). Impulse control disorders in REM sleep behavior disorder. *Curr. Treat. Options Neurol.* 21:23. doi: 10.1007/s11940-019-0564-3
- Filip, P., Linhartová, P., Hlavatá, P., Šumec, R., Baláž, M., Bareš, M., et al. (2018). Disruption of multiple distinctive neural networks associated with impulse control disorder in Parkinson's disease. *Front. Hum. Neurosci.* 12:462. doi: 10.3389/fnhum.2018.00462
- Fox, M. D. (2018). Mapping symptoms to brain networks with the human connectome. *N. Engl. J. Med.* 379, 2237–2245. doi: 10.1056/NEJMra1706158
- Frosini, D., Pesaresi, I., Cosottini, M., Belmonte, G., Rossi, C., Dell'Osso, L., et al. (2010). Parkinson's disease and pathological gambling: results from a functional MRI study. *Mov. Disord.* 25, 2449–2453. doi: 10.1002/mds.23369
- Gan, C., Wang, L., Ji, M., Ma, K., Sun, H., Zhang, K., et al. (2021). Abnormal interhemispheric resting state functional connectivity in Parkinson's disease patients with impulse control disorders. *NPJ Parkinsons Dis.* 7:60. doi: 10.1038/s41531-021-00205-7
- Geranmayeh, F., Brownsett, S. L., and Wise, R. J. (2014). Task-induced brain activity in aphasic stroke patients: what is driving recovery? *Brain* 137, 2632–2648. doi: 10.1093/brain/awu163
- Goldstein, R. Z., and Volkow, N. D. (2011). Dysfunction of the prefrontal cortex in addiction: neuroimaging findings and clinical implications. *Nat. Rev. Neurosci.* 12, 652–669. doi: 10.1038/nrn3119
- Grahn, J. A., Parkinson, J. A., and Owen, A. M. (2009). The role of the basal ganglia in learning and memory: neuropsychological studies. *Behav. Brain Res.* 199, 53–60. doi: 10.1016/j.bbr.2008.11.020
- Grassi, G., Albani, G., Terenzi, F., Razzolini, L., and Ramat, S. (2021). New pharmacological and neuromodulation approaches for impulsive-compulsive behaviors in Parkinson's disease. *Neurol. Sci.* 42, 2673–2682. doi: 10.1007/s10072-021-05237-8
- Hepp, D. H., Foncke, E. M. J., Olde Dubbelink, K. T. E., van de Berg, W. D. J., Berendse, H. W., and Schoonheim, M. M. (2017). Loss of functional connectivity in patients with Parkinson disease and visual hallucinations. *Radiology* 285, 896–903. doi: 10.1148/radiol.2017170438
- Huang, X., Li, B., Li, Y., Lin, J., Shang, H., and Yang, J. (2023). A multimodal meta-analysis of gray matter alterations in trigeminal neuralgia. *Front. Neurol.* 14:1179896. doi: 10.3389/fneur.2023.1179896
- Ji, J. L., Spronk, M., Kulkarni, K., Repovš, G., Anticevic, A., and Cole, M. W. (2019). Mapping the human brain's cortical-subcortical functional network organization. *NeuroImage* 185, 35–57. doi: 10.1016/j.neuroimage.2018.10.006
- Joutsa, J., Moussawi, K., Siddiqi, S. H., Abdolahi, A., Drew, W., Cohen, A. L., et al. (2022). Brain lesions disrupting addiction map to a common human brain circuit. *Nat. Med.* 28, 1249–1255. doi: 10.1038/s41591-022-01834-y
- Kelly, M. J., Baig, F., Hu, M. T., and Okai, D. (2020). Spectrum of impulse control behaviours in Parkinson's disease: pathophysiology and management. *J. Neurol. Neurosurg. Psychiatry* 91, 703–711. doi: 10.1136/jnnp-2019-322453
- Kim, N. Y., Hsu, J., Talmasov, D., Joutsa, J., Soussand, L., Wu, O., et al. (2021). Lesions causing hallucinations localize to one common brain network. *Mol. Psychiatry* 26, 1299–1309. doi: 10.1038/s41380-019-0565-3
- Kimura, I., Revankar, G. S., Ogawa, K., Amano, K., Kajiyama, Y., Mochizuki, H., et al. (2023). Neural correlates of impulsive compulsive behaviors in Parkinson's disease: A Japanese retrospective study. *Neuroimage Clin.* 37:103307. doi: 10.1016/j.nicl.2022.103307
- Kletenik, I., Ferguson, M. A., Bateman, J. R., Cohen, A. L., Lin, C., Tetreault, A., et al. (2022). Network localization of unconscious visual perception in Blindsight. *Ann. Neurol.* 91, 217–224. doi: 10.1002/ana.26292
- Koob, G. F., and Volkow, N. D. (2016). Neurobiology of addiction: a neurocircuitry analysis. *Lancet Psychiatry* 3, 760–773. doi: 10.1016/s2215-0366(16)00104-8
- Latella, D., Maggio, M. G., Maresca, G., Saporoso, A. F., Le Cause, M., Manuli, A., et al. (2019). Impulse control disorders in Parkinson's disease: a systematic review on risk factors and pathophysiology. *J. Neurol. Sci.* 398, 101–106. doi: 10.1016/j.jns.2019.01.034
- Lee, J. Y., Seo, S. H., Kim, Y. K., Yoo, H. B., Kim, Y. E., Song, I. C., et al. (2014). Extrastriatal dopaminergic changes in Parkinson's disease patients with impulse control disorders. *J. Neurol. Neurosurg. Psychiatry* 85, 23–30. doi: 10.1136/jnnp-2013-305549
- Liao, W., Zhang, Z., Pan, Z., Mantini, D., Ding, J., Duan, X., et al. (2011). Default mode network abnormalities in mesial temporal lobe epilepsy: a study combining fMRI and DTI. *Hum. Brain Mapp.* 32, 883–895. doi: 10.1002/hbm.21076
- Lin, J., Li, L., Pan, N., Liu, X., Zhang, X., Suo, X., et al. (2023). Neural correlates of neuroticism: a coordinate-based meta-analysis of resting-state functional brain imaging studies. *Neurosci. Biobehav. Rev.* 146:105055. doi: 10.1016/j.neubiorev.2023.105055

- London, E. D. (2020). Human brain imaging links dopaminergic systems to impulsivity. *Curr. Top. Behav. Neurosci.* 47, 53–71. doi: 10.1007/7854_2019_125
- Long, D., Wang, J., Xuan, M., Gu, Q., Xu, X., Kong, D., et al. (2012). Automatic classification of early Parkinson's disease with multi-modal MR imaging. *PLoS One* 7:e47714. doi: 10.1371/journal.pone.0047714
- Ma, N., Liu, Y., Fu, X. M., Li, N., Wang, C. X., Zhang, H., et al. (2011). Abnormal brain default-mode network functional connectivity in drug addicts. *PLoS One* 6:e16560. doi: 10.1371/journal.pone.0016560
- Maggi, G., Loayza, F., Vitale, C., Santangelo, G., and Obeso, I. (2024). Anatomical correlates of apathy and impulsivity co-occurrence in early Parkinson's disease. *J. Neurol.* 271, 2798–2809. doi: 10.1007/s00415-024-12233-3
- Marques, A., Roquet, D., Matar, E., Taylor, N. L., Pereira, B., O'Callaghan, C., et al. (2021). Limbic hypoconnectivity in idiopathic REM sleep behaviour disorder with impulse control disorders. *J. Neurol.* 268, 3371–3380. doi: 10.1007/s00415-021-10498-6
- Martinez, E., Pasquereau, B., Saga, Y., Météreau, É., and Tremblay, L. (2020). The anterior caudate nucleus supports impulsive choices triggered by pramipexole. *Mov. Disord.* 35, 296–305. doi: 10.1002/mds.27898
- Meyer, G. M., Spay, C., Beliakova, A., Gaugain, G., Pezzoli, G., Ballanger, B., et al. (2020). Inhibitory control dysfunction in parkinsonian impulse control disorders. *Brain* 143, 3734–3747. doi: 10.1093/brain/awaa318
- Meyer, G. M., Spay, C., Laurencin, C., Ballanger, B., Sescousse, G., and Boulinguez, P. (2019). Functional imaging studies of impulse control disorders in Parkinson's disease need a stronger neurocognitive footing. *Neurosci. Biobehav. Rev.* 98, 164–176. doi: 10.1016/j.neubiorev.2019.01.008
- Milardi, D., Quartarone, A., Bramanti, A., Anastasi, G., Bertino, S., Basile, G. A., et al. (2019). The Cortico-basal ganglia-cerebellar network: past, present and future perspectives. *Front. Syst. Neurosci.* 13:61. doi: 10.3389/fnsys.2019.00061
- Mo, F., Zhao, H., Li, Y., Cai, H., Song, Y., Wang, R., et al. (2024). Network localization of state and trait of auditory verbal hallucinations in schizophrenia. *Schizophr. Bull.* 50, 1326–1336. doi: 10.1093/schbul/sbae020
- Moegle, C., Grillon, A., Anheim, M., Lipsker, D., and Velter, C. (2020). Impulse control disorder-linked hypersexuality complicated by disseminated gonococcal infection in a patient with Parkinson's disease. *Rev. Neurol.* 176, 292–293. doi: 10.1016/j.neuro.2019.10.007
- Moher, D., Liberati, A., Tetzlaff, J., and Altman, D. G. (2009). Preferred reporting items for systematic reviews and meta-analyses: the PRISMA statement. *PLoS Med.* 6:e1000097. doi: 10.1371/journal.pmed.1000097
- Morese, R., and Palermo, S. (2020). Altruistic punishment and impulsivity in Parkinson's disease: a social neuroscience perspective. *Front. Behav. Neurosci.* 14:102. doi: 10.3389/fnbeh.2020.00102
- Müller, V. I., Cieslik, E. C., Laird, A. R., Fox, P. T., Radua, J., Mataix-Cols, D., et al. (2018). Ten simple rules for neuroimaging meta-analysis. *Neurosci. Biobehav. Rev.* 84, 151–161. doi: 10.1016/j.neubiorev.2017.11.012
- Murphy, K., and Fox, M. D. (2017). Towards a consensus regarding global signal regression for resting state functional connectivity MRI. *NeuroImage* 154, 169–173. doi: 10.1016/j.neuroimage.2016.11.052
- Paz-Alonso, P. M., Navalpotro-Gomez, I., Boddy, P., Dacosta-Aguayo, R., Delgado-Alvarado, M., Quiroga-Varela, A., et al. (2020). Functional inhibitory control dynamics in impulse control disorders in Parkinson's disease. *Mov. Disord.* 35, 316–325. doi: 10.1002/mds.27885
- Peng, S., Xu, P., Jiang, Y., and Gong, G. (2022). Activation network mapping for integration of heterogeneous fMRI findings. *Nat. Hum. Behav.* 6, 1417–1429. doi: 10.1038/s41562-022-01371-1
- Petersen, K., Van Wouwe, N., Stark, A., Lin, Y. C., Kang, H., Trujillo-Diaz, P., et al. (2018). Ventral striatal network connectivity reflects reward learning and behavior in patients with Parkinson's disease. *Hum. Brain Mapp.* 39, 509–521. doi: 10.1002/hbm.23860
- Premi, E., Pilotto, A., Garibotto, V., Bigni, B., Turrone, R., Alberici, A., et al. (2016). Impulse control disorder in PD: A lateralized monoaminergic frontostriatal disconnection syndrome? *Parkinsonism Relat. Disord.* 30, 62–6. doi: 10.1016/j.parkreldis.2016.05.028
- Probst, C. C., and van Eimeren, T. (2013). The functional anatomy of impulse control disorders. *Curr. Neurol. Neurosci. Rep.* 13:386. doi: 10.1007/s11910-013-0386-8
- Qiu, X., He, Z., Cao, X., and Zhang, D. (2023). Transcranial magnetic stimulation and transcranial direct current stimulation affect explicit but not implicit emotion regulation: a meta-analysis. *Behav. Brain Funct.* 19:15. doi: 10.1186/s12993-023-00217-8
- Rao, H., Mamikonyan, E., Detre, J. A., Siderowf, A. D., Stern, M. B., Potenza, M. N., et al. (2010). Decreased ventral striatal activity with impulse control disorders in Parkinson's disease. *Mov. Disord.* 25, 1660–9. doi: 10.1002/mds.23147
- Ray, N. J., Miyasaki, J. M., Zurovsky, M., Ko, J. H., Cho, S. S., Pellicchia, G., et al. (2012). Extrastriatal dopaminergic abnormalities of DA homeostasis in Parkinson's patients with medication-induced pathological gambling: a [11C]FLB-457 and PET study. *Neurobiol. Dis.* 48, 519–25. doi: 10.1016/j.nbd.2012.06.021
- Reimann, G. M., Küppers, V., Camilleri, J. A., Hoffstaedter, F., Langner, R., Laird, A. R., et al. (2023). Convergent abnormality in the subgenual anterior cingulate cortex in insomnia disorder: a revisited neuroimaging meta-analysis of 39 studies. *Sleep Med. Rev.* 71:101821. doi: 10.1016/j.smrv.2023.101821
- Roussakis, A. A., Lao-Kaim, N. P., and Piccini, P. (2019). Brain imaging and impulse control disorders in Parkinson's disease. *Curr. Neurol. Neurosci. Rep.* 19:67. doi: 10.1007/s11910-019-0980-5
- Santangelo, G., Raimo, S., Cropano, M., Vitale, C., Barone, P., and Trojano, L. (2019). Neural bases of impulse control disorders in Parkinson's disease: a systematic review and an ALE meta-analysis. *Neurosci. Biobehav. Rev.* 107, 672–685. doi: 10.1016/j.neubiorev.2019.09.041
- Seghier, M. L. (2013). The angular gyrus: multiple functions and multiple subdivisions. *Neuroscientist* 19, 43–61. doi: 10.1177/1073858412440596
- Seghier, M. L. (2023). Multiple functions of the angular gyrus at high temporal resolution. *Brain Struct. Funct.* 228, 7–46. doi: 10.1007/s00429-022-02512-y
- Šimić, G., Kkalčić, M., Vukić, V., Mulc, D., Španić, E., Šagud, M., et al. (2021). Understanding emotions: origins and roles of the amygdala. *Biomol. Ther.* 11:823. doi: 10.3390/biom11060823
- Smith, C. T., San Juan, M. D., Dang, L. C., Katz, D. T., Perkins, S. F., Burgess, L. L., et al. (2018). Ventral striatal dopamine transporter availability is associated with lower trait motor impulsivity in healthy adults. *Transl. Psychiatry* 8:269. doi: 10.1038/s41398-018-0328-y
- Sonuga-Barke, E. J., and Castellanos, F. X. (2007). Spontaneous attentional fluctuations in impaired states and pathological conditions: a neurobiological hypothesis. *Neurosci. Biobehav. Rev.* 31, 977–986. doi: 10.1016/j.neubiorev.2007.02.005
- Spreng, R. N., Mar, R. A., and Kim, A. S. (2009). The common neural basis of autobiographical memory, prospection, navigation, theory of mind, and the default mode: a quantitative meta-analysis. *J. Cogn. Neurosci.* 21, 489–510. doi: 10.1162/jocn.2008.21029
- Staubo, S. C., Fuskevåg, O. M., Toft, M., Lie, I. H., Alvik, K. M. J., Jostad, P., et al. (2024). Dopamine agonist serum concentrations and impulse control disorders in Parkinson's disease. *Eur. J. Neurol.* 31:e16144. doi: 10.1111/ene.16144
- Tessitore, A., De Micco, R., Giordano, A., di Nardo, F., Caiazzo, G., Siciliano, M., et al. (2017a). Intrinsic brain connectivity predicts impulse control disorders in patients with Parkinson's disease. *Mov. Disord.* 32, 1710–1719. doi: 10.1002/mds.27139
- Tessitore, A., Santangelo, G., De Micco, R., Giordano, A., Raimo, S., Amboni, M., et al. (2017b). Resting-state brain networks in patients with Parkinson's disease and impulse control disorders. *Cortex* 94, 63–72. doi: 10.1016/j.cortex.2017.06.008
- Tetreault, A. M., Phan, T., Orlando, D., Lyu, I., Kang, H., Landman, B., et al. (2020). Network localization of clinical, cognitive, and neuropsychiatric symptoms in Alzheimer's disease. *Brain* 143, 1249–1260. doi: 10.1093/brain/awaa058
- Theis, H., Probst, C., Campabadal, A., Goerlich, K. S., Granert, O., Wolff, S., et al. (2022). Inhibitory framing in hypersexual patients with Parkinson's disease. An fMRI pilot study. *Exp. Brain Res.* 240, 2097–2107. doi: 10.1007/s00221-022-06397-5
- Toś, M., Grażyńska, A., Antoniuk, S., and Siuda, J. (2023). Impulse control disorders in the polish population of patients with Parkinson's disease. *Medicina* 59:468. doi: 10.3390/medicina59081468
- van Eimeren, T., Ballanger, B., Pellicchia, G., Miyasaki, J. M., Lang, A. E., and Strafella, A. P. (2009). Dopamine agonists diminish value sensitivity of the orbitofrontal cortex: a trigger for pathological gambling in Parkinson's disease? *Neuropsychopharmacology* 34, 2758–2766. doi: 10.1038/npp.2009.124
- Van Essen, D. C., Smith, S. M., Barch, D. M., Behrens, T. E., Yacoub, E., and Ugurbil, K. (2013). The WU-Minn human connectome project: an overview. *NeuroImage* 80, 62–79. doi: 10.1016/j.neuroimage.2013.05.041
- Verger, A., Klesse, E., Chawki, M. B., Witjas, T., Azulay, J. P., Eusebio, A., et al. (2018). Brain PET substrate of impulse control disorders in Parkinson's disease: A metabolic connectivity study. *Hum. Brain Mapp.* 39, 3178–3186. doi: 10.1002/hbm.24068
- Vitale, C., Amboni, M., Erro, R., Picillo, M., Pellicchia, M. T., Barone, P., et al. (2019). Parkinson's disease management and impulse control disorders: current state and future perspectives. *Expert. Rev. Neurother.* 19, 495–508. doi: 10.1080/14737175.2019.1620603
- Voon, V., Napier, T. C., Frank, M. J., Sgambato-Faure, V., Grace, A. A., Rodriguez-Oroz, M., et al. (2017). Impulse control disorders and levodopa-induced dyskinesias in Parkinson's disease: an update. *Lancet Neurol.* 16, 238–250. doi: 10.1016/s1474-4422(17)30004-2
- Voon, V., Sohr, M., Lang, A. E., Potenza, M. N., Siderowf, A. D., Whetteckey, J., et al. (2011). Impulse control disorders in Parkinson disease: a multicenter case-control study. *Ann. Neurol.* 69, 986–996. doi: 10.1002/ana.22356
- Wagle Shukla, A., Shuster, J. J., Chung, J. W., Vaillancourt, D. E., Patten, C., Ostrem, J., et al. (2016). Repetitive transcranial magnetic stimulation (rTMS) therapy in Parkinson disease: a meta-analysis. *PMR* 8, 356–366. doi: 10.1016/j.pmrj.2015.08.009
- Wang, L., Shen, H., Lei, Y., Zeng, L. L., Cao, F., Su, L., et al. (2017). Altered default mode, fronto-parietal and salience networks in adolescents with internet addiction. *Addict. Behav.* 70, 1–6. doi: 10.1016/j.addbeh.2017.01.021
- Wawrzyniak, M., Klingbeil, J., Zeller, D., Saur, D., and Classen, J. (2018). The neuronal network involved in self-attribution of an artificial hand: a lesion network-mapping study. *NeuroImage* 166, 317–324. doi: 10.1016/j.neuroimage.2017.11.011
- Weintraub, D., David, A. S., Evans, A. H., Grant, J. E., and Stacy, M. (2015). Clinical spectrum of impulse control disorders in Parkinson's disease. *Mov. Disord.* 30, 121–127. doi: 10.1002/mds.26016

- Williams, W. A., and Potenza, M. N. (2008). The neurobiology of impulse control disorders. *Braz J Psychiatry* 30, S24–S30. doi: 10.1590/s1516-44462008005000003
- Yan, C. G., Wang, X. D., Zuo, X. N., and Zang, Y. F. (2016). DPABI: data processing & analysis for (resting-state) brain imaging. *Neuroinformatics* 14, 339–351. doi: 10.1007/s12021-016-9299-4
- Yeo, B. T., Krienen, F. M., Sepulcre, J., Sabuncu, M. R., Lashkari, D., Hollinshead, M., et al. (2011). The organization of the human cerebral cortex estimated by intrinsic functional connectivity. *J. Neurophysiol.* 106, 1125–1165. doi: 10.1152/jn.00338.2011
- Zhang, J. F., Wang, X. X., Feng, Y., Fekete, R., Jankovic, J., and Wu, Y. C. (2021). Impulse control disorders in Parkinson's disease: epidemiology, pathogenesis and therapeutic strategies. *Front. Psych.* 12:635494. doi: 10.3389/fpsy.2021.635494
- Zhang, J., Wu, X., Si, Y., Liu, Y., Wang, X., Geng, Y., et al. (2024). Abnormal caudate nucleus activity in patients with depressive disorder: Meta-analysis of task-based functional magnetic resonance imaging studies with behavioral domain. *Psychiatry Res. Neuroimaging* 338:111769. doi: 10.1016/j.psychres.2023.111769
- Zhang, X., Xu, R., Ma, H., Qian, Y., and Zhu, J. (2024). Brain structural and functional damage network localization of suicide. *Biol. Psychiatry* 95, 1091–1099. doi: 10.1016/j.biopsych.2024.01.003
- Zhu, X., Liu, L., Xiao, Y., Li, F., Huang, Y., Han, D., et al. (2021). Abnormal topological network in Parkinson's disease with impulse control disorders: a resting-state functional magnetic resonance imaging study. *Front. Neurosci.* 15:651710. doi: 10.3389/fnins.2021.651710
- Zilverstand, A., Huang, A. S., Alia-Klein, N., and Goldstein, R. Z. (2018). Neuroimaging impaired response inhibition and salience attribution in human drug addiction: a systematic review. *Neuron* 98, 886–903. doi: 10.1016/j.neuron.2018.03.048
- Zsidó, A. N., Darnai, G., Inhof, O., Perlaki, G., Orsi, G., Nagy, S. A., et al. (2019). Differentiation between young adult internet addicts, smokers, and healthy controls by the interaction between impulsivity and temporal lobe thickness. *J. Behav. Addict.* 8, 35–47. doi: 10.1556/2006.8.2019.03

Glossary

ACC - anterior cingulate cortex	HS - hypersexuality
ALFF - amplitude of low-frequency fluctuation	ICA - independent component analysis
ASL - arterial spin labeling	ICB - Impulse control behaviors
BE - binge-eating	ICDs - impulse control disorders
BOLD - blood-oxygen-level-dependent	MRI - magnetic resonance imaging
CBF - cerebral blood flow	MMSE - Mini-Mental State Examination
CE - compulsive eating	MoCA - Montreal Cognitive Assessment
CS - compulsive buying	NA - not applicable
DAN - dorsal attention network	PG - pathological gambling
DBM - deformation-based morphometry	PD - Parkinson's disease
DC - degree centrality	PET - positron emission tomography
DMN - default mode network	ROI - region of interest
DPABI - Data Processing and Analysis of Brain Imaging	rTMS - repetitive transcranial magnetic stimulation
FA - flip angle	rs-fMRI - resting-state functional magnetic resonance imaging
fALFF - fractional amplitude of low-frequency fluctuation	ReHo - regional homogeneity
FC - functional connectivity	rCBF - regional cerebral blood flow
FCNM - functional connectivity network mapping	SPECT - single photon emission computed tomography
fMRI - functional MRI	SPM - Statistical Parametric Mapping
FDR - false discovery rate	TE - echo time
FWE - family-wise error	TR - repetition time
FOV - field of view	UPDRS - Unified Parkinson's disease rating scale
GRE-EPI - gradient-recalled echo-planar imaging	VBM - voxel-based morphometry
GMV - gray matter volume	VMHC - voxel-mirrored homotopic connectivity